Acta Cryst. (1994). B**50**, 307–312

Crystal Structure of β-$Al_{4.5}FeSi$

BY CHR. RØMMING

Department of Chemistry, University of Oslo, PO Box 1033 *Blindern*, 0315 *Oslo, Norway*

AND V. HANSEN AND J. GJØNNES

Department of Physics, University of Oslo, PO Box 1048 *Blindern*, 0316 *Oslo, Norway*

(*Received* 6 *July* 1993; *accepted* 23 *November* 1993)

Abstract

By a combination of X-ray and electron diffraction, the average structure of the intermetallic phase β-$Al_{4.5}FeSi$ has been determined. The crystals grown from the melt were generally of poor quality; the monoclinic space group $A2/a$ was deduced from electron diffraction patterns obtained from small domains. X-ray diffraction data measured at T = 298 K with Mo $K\alpha$ radiation (λ = 0.71069 Å) out to $\sin\theta/\lambda = 0.8$ Å^{-1} resulted in 1739 observed reflections, of which 980 were unique. Of these, 244 weak reflections affected by disorder were removed. Cell dimensions are a = 6.161 (3), b = 6.175 (3), c = 20.813 (6) Å, β = 90.42 (3)°. As indicated by the chemical composition there are eight Fe and 44 Al/Si atoms in the unit cell. The average structure was determined by direct methods and refined to a conventional R factor of 0.039. The structure may be described in terms of ten-coordinated iron in the centre of a double-capped square antiprism of Al/Si atoms, which again are joined together in double layers normal to the c axis by the sharing of antiprism edges in the layer and cap atoms between the two single layers.

Introduction

The intermetallic phase β-$Al_{4.5}FeSi$ was first identified in the ternary Al–Fe–Si alloy system by Rosenhain, Archbutt & Hanson (1921) and originally called the X phase. The composition was determined by several workers and found to correspond closely to $Al_{4.5}FeSi$ (Black, 1954). Despite its common occurrence in industrial aluminium alloys, the crystal structure has not previously been determined, presumably due to poor crystal quality; single crystals grown from the melt contain many faults and are, as a rule, not well suited for structure analysis by X-ray diffraction. This may explain the variation in the unit-cell parameters quoted in the literature. Most workers report a monoclinic unit cell: $a \simeq 6.12$, $b \simeq 6.12$, $c \simeq 41.5$ Å, $\beta \simeq 91°$ (Phragmén, 1950), whereas Black (1954) in a series of structural studies of Al–Fe–Si phases reported $4m$ symmetry from Laue photographs and proposed a tetragonal cell with a = 6.18, c = 42.5 Å for the β phase.

The phase is frequently noted in electron microscopy studies of industrial alloys. Høier, Lohne & Mørtvedt (1977) described their patterns in terms of a monoclinic unit cell with parameters $a \simeq 6.18$, $b \simeq 6.18$, $c \simeq 20.8$ Å, $\beta \simeq 91°$ and interpreted the diffuse scattering in terms of multiple twins on (001) planes. Recently Carpenter & Le Page (1993) proposed an orthorhombic B-centred cell with a = 6.18, b = 6.25 and c = 20.69 Å from convergent beam electron diffraction (CBED) patterns.

In the present investigation single crystals were grown from a melt of composition 2 wt% Fe, 10 wt% Si and 88 wt% Al. An extensive electron diffraction study was carried out in order to characterize the unit cell, symmetries and faults before attempts to determine the crystal structure with single-crystal X-ray methods were carried out. This combination of methods proved essential to solve the structure.

Experimental

Preparations

Crystals of β-$Al_{4.5}FeSi$ were grown from a melt. 8.8 g of aluminium chips of 99.99 wt% purity, 0.2 g iron wire and 1.0 g silicon were mixed together in an alumina crucible and covered by cryolite. The mixture was enclosed in a quartz ampoule and evacuated before heating to 1373 K and slowly cooled to room temperature. The crystals best suited for X-ray diffraction were obtained by a three-interval cooling program. From 1373 to 973 K the temperature was lowered by 1 K min^{-1}. In the next interval, which is the crucial one, the temperature was changed by only 0.1 K min^{-1} until 773 K was reached. The power was then switched off and the specimen cooled to room temperature in the furnace.

ISSN 0108-7681

The excess aluminium was subsequently dissolved electrolytically in a dilute acid solution with H_2O:HCl:HNO_3 in the molar ratio 1000:1:1, and a nickel strip as the cathode. The crystals obtained were quite large square platelets with characteristic dimensions $2 \times 2 \times 0.1$ mm, see the optical micrograph in Fig. 1. Growth directions ⟨110⟩ and ⟨100⟩ were determined from X-ray photographs.

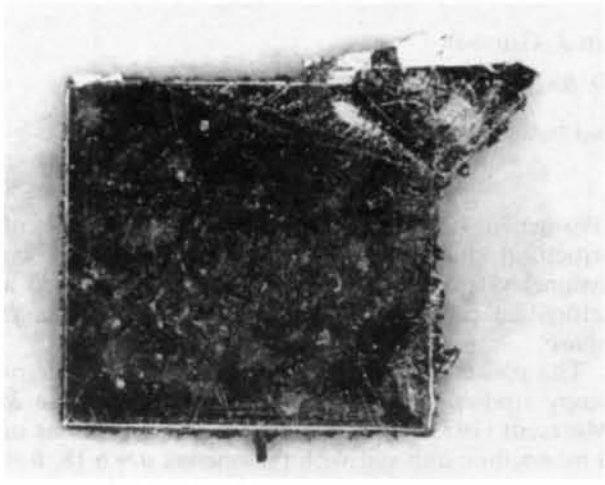

Fig. 1. Optical micrograph of an extracted particle, flattened on (001).

Electron diffraction

Specimens for transmission electron microscopy were prepared by two different routes. Usually the extracted particles were crushed in an agate mortar and small crystallites collected on a supporting holey carbon film. In a few cases the specimens were mechanically ground before thinning in an argon ion beam miller. Electron microscopy examinations were carried out using JEOL 200 CX and JEOL 2000 FX instruments. Both were equipped with energy dispersive X-ray analysis systems; the spectroscopic analyses confirmed the composition reported in the literature.

A number of parallel beam (SAD) and convergent beam electron diffraction patterns were taken in order to confirm the unit cell, to identify faults and to determine the space group (Figs. 2 and 3). The patterns were consistent with the cell reported in the literature, *viz.* $a \simeq b \simeq 6.18$ Å and a c axis of 20.8 Å. The diffraction patterns and micrographs revealed frequent faults; the domains seen in Fig. 4 were identified as twins on (001). The separation along c^*

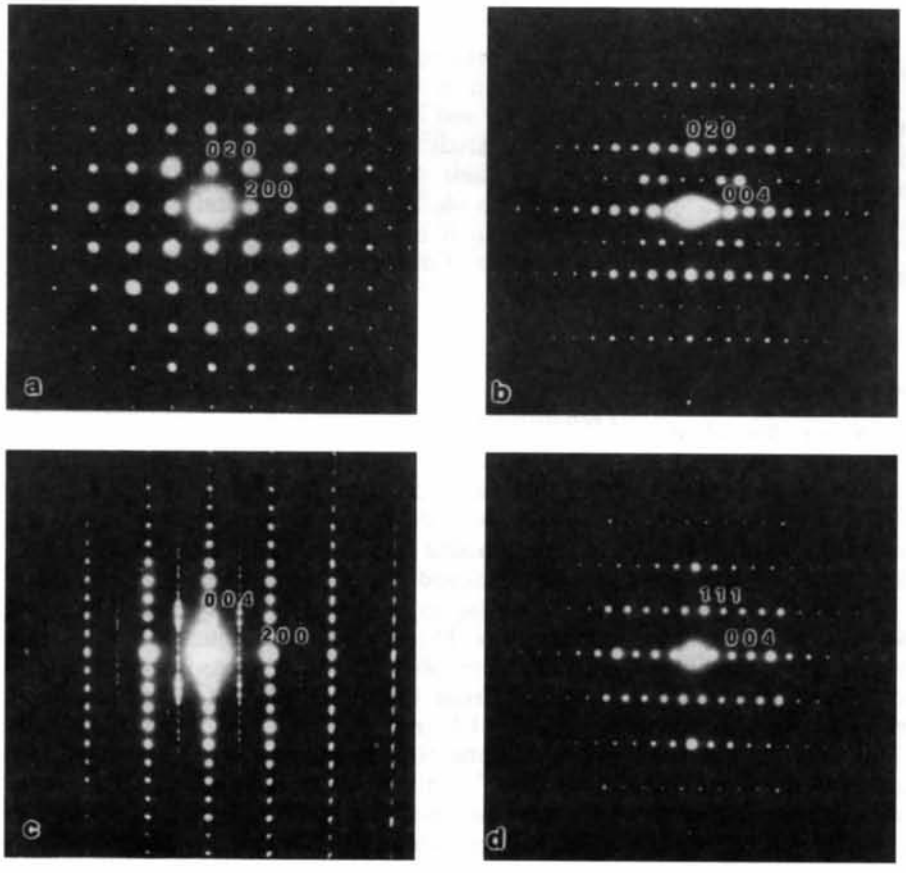

Fig. 2. Electron diffraction patterns from the β-phase: (*a*) [001] projection, (*b*) [100] projection, (*c*) [010] projection and (*d*) [1$\bar{1}$0] projection.

between the matrix and twin spots was measured in the $h0l$ patterns, *e.g.* on the $60l$ line in Fig. 2(*c*), and was found to be consistent with the β angle near 90.5°. Diffuse c^* streaks and spots with $h = 2n + 1$, $k = 2n$ are often seen as in Fig. 2(*c*); these are associated with multiple twins.

The dimensions of the monoclinic unit cell, which is nearly tetragonal, complicate the electron diffraction observations in various ways. At the microscope it may be impossible in practice to distinguish between the a^* and b^* axes in diffraction patterns, since the two are almost equal in length, see Figs. 2 and 3. A further complication is added by the existence of domains with a and b interchanged. The (001) twin faults offer a possibility for identification of the orientation of such domains. Fig. 2(*c*) is thus clearly identified as a [010] projection by the diffuse streaks parallel to c^* for $h = 2n + 1$, since no such streaks will appear in a [100] projection. The configuration of spots and streaks in reciprocal space is illustrated in Fig. 5.

An A-centred unit cell was concluded from the absence of reflections with $k + l = 2n + 1$, except in the [001] projection (Fig. 2*a*) where weak reflections

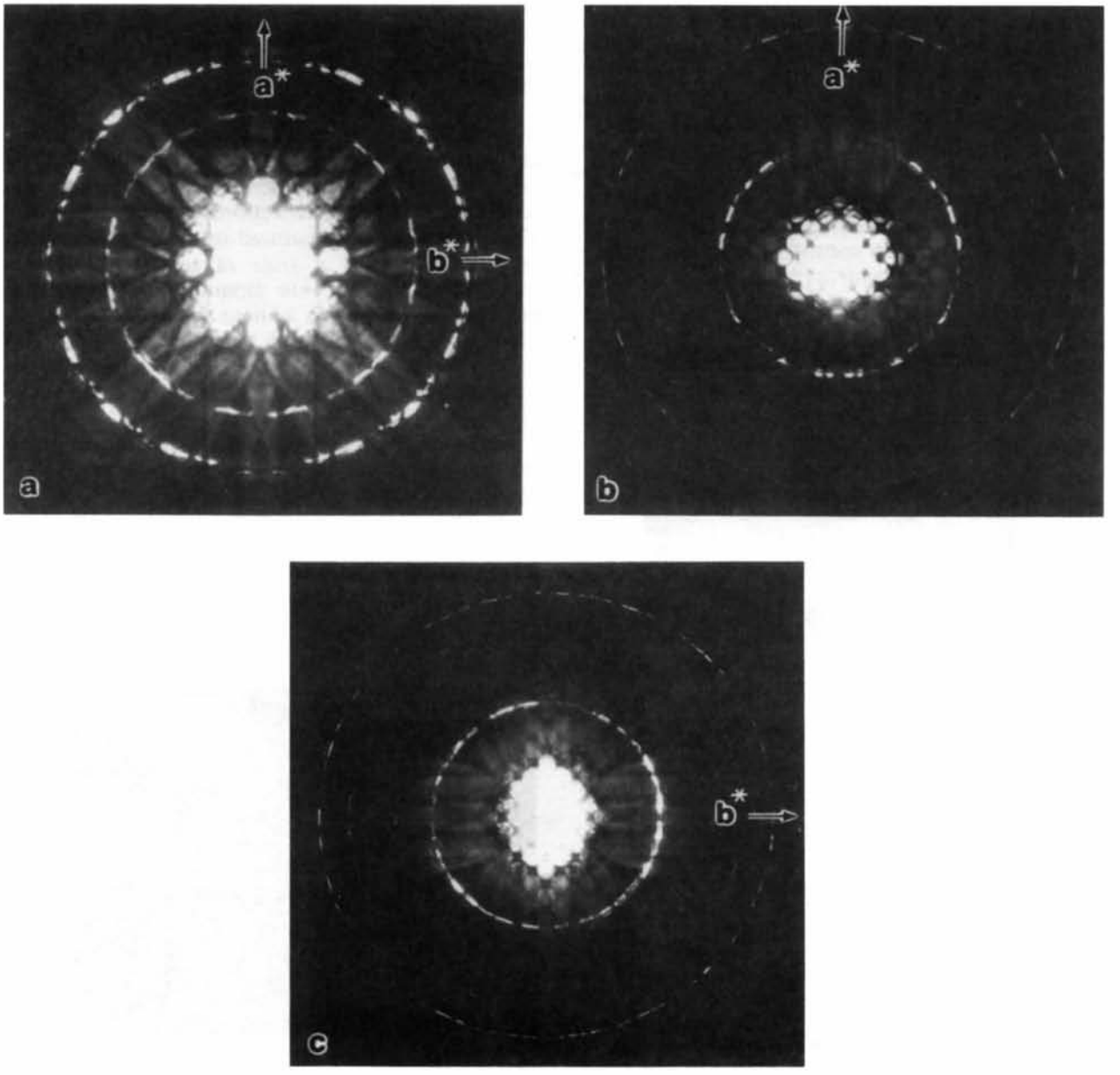

Fig. 3. CBED patterns from the β-phase: (*a*) [001] projection, (*b*) [101] projection and (*c*) [011] projection.

with $k = 2n + 1$ appeared. These can be attributed to diffuse streaks parallel to c^* by an apparent lower symmetry caused by a fractional number of unit cells in the c direction along the foil normal – or by interchange of a and b axes.

CBED patterns taken near the [001] axis, Fig. 3, appear at first to have fourfold symmetry, but close inspection reveals (010) mirror symmetry only; across (100) there is slight deviation from reflection symmetry confirmed by tilting towards the [101] and [011] projections, as expected for a monoclinic unit cell. Systematic absences other than those which follow from the A-centre were difficult to ascertain, owing to a combination of diffuse streaks and double diffraction effects. The reflection symmetry across (010) may be due to a glide plane. SAD and CBED patterns were therefore taken in several projections. In order to look for an a glide, crystals were systematically tilted away from [001] around a^* and b^*, respectively, to [201] and [021], Fig. 6(*a*) and 6(*b*). The absence of $(10\bar{2})$ reflection is clearly seen in the [201] projection. By using a small selection aperture in order to avoid twinned regions we also succeeded in observing extinction consistent with an a glide in ($h0l$), Fig. 6(*c*). The centrosymmetrical space group $A2/a$ was therefore assumed to be correct for the structure determination.

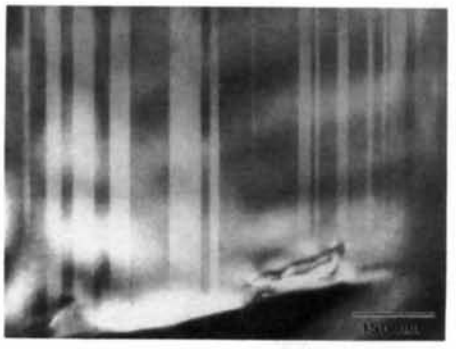

Fig. 4. Dark-field image of twins, taken with an intense part of the (10l) streak.

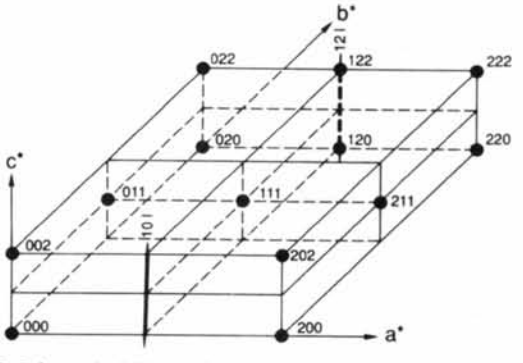

Fig. 5. Schematical illustration of the reciprocal lattice and streaks along the ⟨10l⟩ direction.

X-ray diffraction

Specimens for X-ray structure determination were prepared from the extracted particles and cleaved to suitable dimensions after the removal of surface precipitates of silicon. Well cleaved fragments were fixed at the tip of a glass pin parallel to the c axis. A large number of crystals were checked by oscillation around the c axis in a Weissenberg camera in order to select a single crystal suitable for X-ray diffractometry. Most oscillation photographs indicated poor quality and prolific faults in the crystals; Weissenberg photographs were sometimes taken as a further check when the oscillation photographs indicated few faults.

X-ray intensities were collected on a Nicolet $P/3F$ four-circle diffractometer using graphite monochromatized Mo $K\alpha$ radiation ($\lambda = 0.71069$ Å). The lattice parameters were determined from the accurate settings of 25 general reflections with $31 < 2\theta < 42°$. The intensities were measured using an ω scan speed of $2.0° \text{ min}^{-1}$ and a scan range of 2.8°. Three standard reflections were monitored for every 100 intensity measurements without significant variation. The size of the crystal was approximately $300 \times 200 \times 70$ μm. Data were collected at 293 K from a hemisphere of reciprocal space within $\sin\theta/\lambda = 0.8$ Å^{-1} for $0 < h < 12$, $-17 < k < 17$ and $-35 < l \leq 35$.

Assuming the space group $A2/a$ determined in the electron diffraction experiments to be correct [$A2/a$; equivalent positions (0,0,0, 0,1/2,1/2) + (x, y, z; $-x$, $-y$, $-z$; $1/2 - x$, y, $-z$; $1/2 + x$, $-y$, z)], 1739 observed reflections [$I > 5\sigma(I)$] merged to 980 unique reflections where $\sigma(I)$ is defined by $\sigma^2(I) = P + B + (0.025\,(P - B))^2$, O = scan counts and B = back-

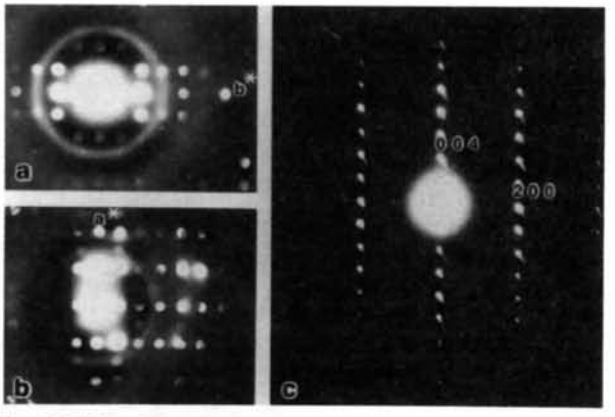

Fig. 6. Diffraction pattern of the β-phase. Note that ($h0l$) reflections are present only where $h = 2n$, $l = 2n$. (*a*) [201] projection, (*b*) [021] projection and (*c*) [010] projection.

Table 1. *Final fractional coordinates with estimated standard deviations and equivalent displacement factors* (Å^3)

$U_{eq} = (1/3)\sum_i \sum_j U_{ij} a_i^* a_j^* \mathbf{a}_i . \mathbf{a}_j .$

	x	y	z	U_{eq}
Fe(1)	0.5024 (1)	0.2605 (5)	0.13671 (3)	0.011
Al(1)	0.3583 (3)	0.6062 (3)	0.1863 (1)	0.016
Al(2)	0.3387 (3)	−0.0884 (3)	0.0897 (1)	0.017
Al(3)	0.1669 (3)	0.4167 (3)	0.0908 (1)	0.018
Al(4)	0.4972 (3)	0.2666 (7)	0.0181 (1)	0.016
Al(5)	0.50000	0.25000	0.25000	0.020
Al(6)	0.1526 (3)	0.1000 (3)	0.1836 (1)	0.015

ground counts. Out of these, the 244 reflections with $h + k = 2n + 1$ were weak and, according to the electron diffraction experiments, severely affected by diffuse streaks owing to twinning and disorder; they were, therefore, removed from the data set. The data were corrected for Lorentz, polarization and absorption effects [empirical absorption correction (Walker & Stuart, 1983)]; based on the structure isotropically refined before merging equivalent reflections, minimum and maximum corrections were 0.707 and 1.259, respectively; $R_{int} = 0.043$. The structure was determined by direct methods [*Mithril* (Gilmore, 1984)] followed by successive Fourier calculations. Final full-matrix least-squares refinements on F [$w = 1/\sigma^2(F)$] included scale, positional and anisotropic thermal parameters and were based on 736 reflections. For the final refinement $R = 0.039$, $wR = 0.049$, $S = 4.11$, $(\Delta/\sigma) < 0.02$, $\Delta\rho_{max} = 0.95$ e Å^{-3} and $\Delta\rho_{min} = -1.52$ e Å^{-3}. Scattering factors were taken from *International Tables for X-ray Crystallography* (1974, Vol IV, Table 2.2B, pp. 99, 101) Final parameters are listed in Table 1.*

Attempts to refine the structure in a tetragonal space group were not successful. The R factor for merging equivalent reflections was 0.14; the refinements yield R factors well above 0.12.

Description of structure

Fig. 7 shows the structure determined for β-$Al_{4.5}FeSi$ as viewed along the [010] direction. The structure is defined by one Fe atom and five Al atoms in general positions and one Al atom (Al5) in a centre of symmetry (Wyckoff position *d*). The Si atom of the net formula $Al_{4.5}FeSi$ could not be distinguished from an Al atom and we assumed that it was statistically distributed among the Al positions. The slightly larger thermal vibrations of the Al atoms compared with those of the Fe atom could also be an indication of this. The resulting average structure may be described by ten-coordinated Fe atoms in the centre of distorted double-capped square antiprisms sharing edges arranged in double layers through apices (Al5) in centres of symmetry. The other apex

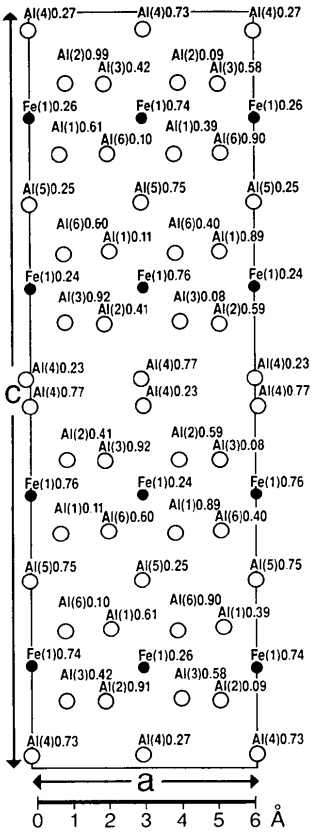

Fig. 7. Projection of the β-$Al_{4.5}FeSi$ structure down the *b* axis.

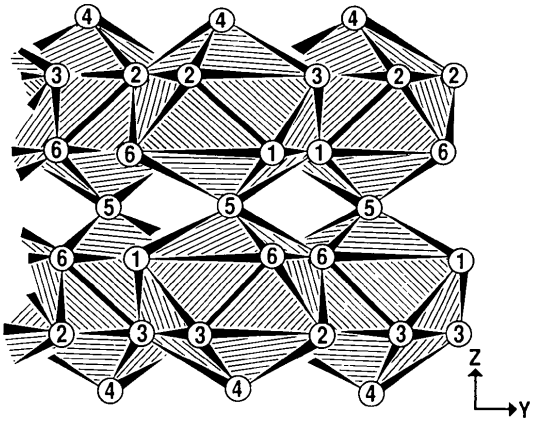

Fig. 8. Schematical illustration of the double layers: Al atoms are indicated by encircled atomic numbering.

* Lists of structure and factors anisotropic thermal parameters have been deposited with the British Library Document Supply Centre as Supplementary Publication No. SUP 71675 (7 pp.). Copies may be obtained through The Technical Editor, International Union of Crystallography, 5 Abbey Square, Chester CH1 2HU, England. [CIF reference: AB0317]

Table 2. *Interatomic distances* (Å) *less than* 3.0 Å *with estimated standard deviations in parentheses*

Fe(1)—Al(1)	2.534 (3)	Fe(1)—Al(1)^{i}	2.553 (2)
Fe(1)—Al(2)	2.596 (3)	Fe(1)—Al(2)^{ii}	2.531 (2)
Fe(1)—Al(3)	2.467 (2)	Fe(1)—Al(3)^{i}	2.434 (3)
Fe(1)—Al(4)	2.468 (1)	Fe(1)—Al(5)	2.358 (1)
Fe(1)—Al(6)	2.572 (2)	Fe(1)—Al(6)^{ii}	2.598 (3)
Al(1)—Al(2)^{iii}	2.758 (3)	Al(1)—Al(3)	2.583 (3)
Al(1)—Al(3)^{i}	2.764 (3)	Al(1)—Al(5)	2.709 (2)
Al(1)—Al(5)^{iv}	2.731 (2)	Al(1)—Al(6)^{v}	2.708 (3)
Al(1)—Al(6)^{i}	2.566 (3)	Al(2)—Al(3)^{ii}	2.863 (3)
Al(2)—Al(4)	2.829 (2)	Al(2)—Al(4)^{vi}	2.702 (2)
Al(2)—Al(4)^{vii}	2.795 (2)	Al(2)—Al(6)	2.553 (3)
Al(2)—Al(6)^{ii}	2.740 (3)	Al(3)—Al(4)	2.708 (2)
Al(3)—Al(4)^{viii}	2.642 (2)	Al(3)—Al(4)^{iv}	2.680 (2)
Al(3)—Al(6)	2.750 (3)	Al(4)—Al(4)^{ix}	2.979 (6)
Al(5)—Al(6)	2.702 (2)	Al(5)—Al(6)^{v}	2.735 (2)

Symmetry codes: (i) $\frac{1}{2}+x$, $1-y$, z; (ii) $\frac{1}{2}+x$, $-y$, z; (iii) x, $1+y$, z; (iv) $-\frac{1}{2}+x$, $1-y$, z; (v) $\frac{1}{2}-x$, $\frac{1}{2}+y$, $\frac{1}{2}-z$; (vi) $1-x$, $-y$, $-z$; (vii) $-\frac{1}{2}+x$, $-y$, z; (viii) $\frac{1}{2}-x$, y, $-z$; (ix) $1-x$, $1-y$, $-z$.

(Al4) binds double layers together through coordination of Al atoms in a neighbouring double layer. The situation is illustrated in Fig. 8. Interatomic distances are listed in Table 2. The Fe—Al distances range from 2.358 (1) to 2.572 (3) Å. The Al—Al distances fall into two groups; the edges shared by two fused square antiprisms, Al(1)—Al(3) and Al(2)—Al(6), are 2.583 (3) and 2.553 (3) Å, respectively. A top edge [Al(1)—Al(6)] of the antiprism is also short, 2.566 (3) Å. The remaining Al—Al distances range from 2.642 to 2.863 Å, except for the long Al(4)—Al(4) bond of 2.979 (6) Å connecting two double layers.

Discussion and conclusions

The structure is based on intensities where h, k, l are all odd or even, the remaining reflections were removed from the data. This systematic elimination of intensities is expected to increase further the tetragonal character of the Fourier, which is evident in several of the electron diffraction patterns, see Fig. 3. Interchange of a and b axes were observed in some electron microscope specimens; this may also occur in the crystal used for intensity collection and thus reduce the intensity difference between reflections of hkl and khl types. It was in fact found that the interchange of a and b axes only slightly affects the X-ray data, with small changes also in the figures of merit. The average structure thus determined appears to be very close to the local structure, with only slight displacement of the atoms away from a tetragonal arrangement.

The coordination polyhedron, the double-capped antiprism, Fig. 9(b), appears with small variations in other Al–(Fe,Mn)–Si structures. *e.g.* as one of two ten-coordinated polyhedra in the α_H-AlFeSi structure (Corby & Black, 1977). In a distorted form it may be recognized also as the most common iron coordination in Al_3Fe (Black, 1955). Five-membered rings of aluminium are a common feature in these structures, emphasizing the close relationship between these polyhedra and the regular 12-atom icosahedron found in $Al_{12}Mn$ and also as a 12-fold coordination in α_H-AlFeSi. If two atoms are removed from this icosahedron, either of the two polyhedra I or II may result by some adjustment of the remaining ten atoms (Fig. 9). Both polyhedra were introduced by Corby & Black in their description of α_H-AlFeSi; II also appears as the coordination of Mn in β-$Al_{4.5}MnSi$ and in Al_6Mn (Robinson, 1952).

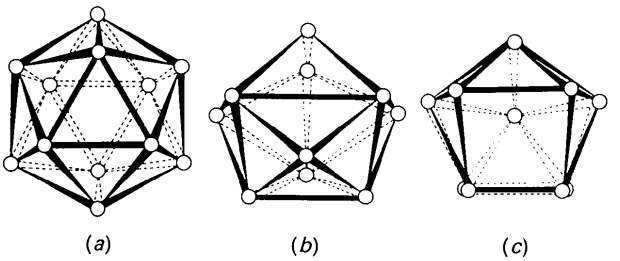

Fig. 9. Related coordination polyhedra in the AlFeSi system (after Corby & Black, 1977): (a) icosahedron with 12 atoms around a central atom; (b) square double-capped antiprism, ten atoms around the central atom (I); (c) alternative way to pack ten atoms around the central atom (II).

CR is grateful to the Norwegian Research Council for Science and Humanities for financial support. The authors thank A. Aasen for technical support.

References

BLACK, P. J. (1954). *Philos. Mag.* **46**, 401–409.
BLACK, P. J. (1955). *Acta Cryst.* **8**, 175–182.
CARPENTER, G. J. C. & LE PAGE, . (1993). *Scr. Metall. Mater.* **28**, 733–736.
CORBY, R. N. & BLACK, P. J. (1977). *Acta Cryst.* B**33**, 3468–3475.
GILMORE, C. J. (1984). *J. Appl. Cryst.* **17**, 42–46.
HØIER, R., LOHNE, O. & MØRTVEDT, S. (1977). *Scand. J. Metall.* **6**, 36–37.
PHRAGMÉN, G. (1950). *J. Inst. Met.* **77**, 489–552.
ROBINSON, K. (1952). *Acta Cryst.* **5**, 397–403.
ROSENHAIN, ARCHBUTT & HANSON (1921). Eleventh Report to the Alloys Research Committee of the Institution of Mechanical Engineers.
WALKER, N. & STUART, D. (1983). *Acta Cryst.* A**39**, 158–166.